BIOCHEMISTRY
including biophysical chemistry & molecular biology

Article

pubs.acs.org/biochemistry

Fully Activated MEK1 Exhibits Compromised Affinity for Binding of Allosteric Inhibitors U0126 and PD0325901

Payal R. Sheth,*[,†] Yuqi Liu,[†] Thomas Hesson,[†] Jia Zhao,[§] Lev Vilenchik,[†] Yan-Hui Liu,[§] Todd W. Mayhood,[†] and Hung V. Le[†]

[†]Protein Science Department and [§]Chemistry Department, Merck Research Laboratories, 2015 Galloping Hill Road, Kenilworth, New Jersey 07033, United States

ABSTRACT: Kinases catalyze the transfer of γ-phosphate from ATP to substrate protein residues triggering signaling pathways responsible for a plethora of cellular events. Isolation and production of homogeneous preparations of kinases in their fully active forms is important for accurate *in vitro* measurements of activity, stability, and ligand binding properties of these proteins. Previous studies have shown that MEK1 can be produced in its active phosphorylated form by coexpression with RAF1 in insect cells. In this study, using activated MEK1 produced by *in vitro* activation by RAF1 (pMEK1$^{in\ vitro}$), we demonstrate that the simultaneous expression of RAF1 for production of activated MEK1 does not result in stoichiometric phosphorylation of MEK1. The pMEK1$^{in\ vitro}$ showed higher specific activity toward ERK2 protein substrate compared to the pMEK1 that was activated via coexpression with RAF1 (pMEK1$^{in\ situ}$). The two pMEK1 preparations showed quantitative differences in the phosphorylation of T-loop residue serine 222 by Western blotting and mass spectrometry. Finally, pMEK1$^{in\ vitro}$ showed marked differences in the ligand binding properties compared to pMEK1$^{in\ situ}$. Contrary to previous findings, pMEK1$^{in\ vitro}$ bound allosteric inhibitors U0126 and PD0325901 with a significantly lower affinity than pMEK1$^{in\ situ}$ as well as its unphosphorylated counterpart (npMEK1) as demonstrated by thermal-shift, AS-MS, and calorimetric studies. The differences in inhibitor binding affinity provide direct evidence that unphosphorylated and RAF1-phosphorylated MEK1 form distinct inhibitor sites.

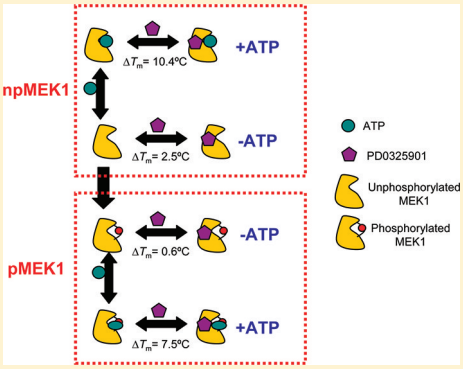

RAF/MEK/ERK is a highly conserved cell-signaling module responsible for several processes including growth, differentiation, and early embryonic development.[1−3] Constitutive activities resulting from aberrant mutations of any components of the module have been associated with malignancies[4,5] and inflammatory diseases.[6] As a result, these kinases of the mitogen-activated protein kinase (MAPK) pathway are excellent targets for pharmacological intervention. The importance of these targets has recently been underscored by encouraging clinical trials results for PLX4032, a BRAF inhibitor highly selective for the V600E mutant.[7] The downstream MAPKK or MEK received no less scrutiny taking into consideration the abundant clinical trials for treatment of cancer with multiple candidate inhibitors.[8−12]

MEK is activated by RAF phosphorylation at serine residues 218 and 222 of the T-loop motif $S_{218}MANS_{222}$.[13,14] Upon activation it acts in turn as a dual specificity kinase to phosphorylate ERK at threonine 183 and tyrosine 185 of the T-loop motif $T_{183}EY_{185}$.[15] The MEK:ERK interaction is exceptionally specific. MEK1/2 kinases are the only known activators of ERK1/2, and ERK1/2 kinases are the only known substrates for MEK1/2. Most MEK inhibitors developed to date for clinical studies are noncompetitive with respect to ATP and bind at an allosteric site distinct from the ATP binding pocket.[16] X-ray crystallography studies of a number of MEK1 inhibitor complexes, especially of those of the PD184352-like series, supported this conclusion.[17,18] Notably, all X-ray crystallography studies of these complexes involved the basal nonphosphorylated form of the enzyme. Fine structural details of the binding of the noncompetitive inhibitors to the phosphorylated and activated form of MEK1 remains to be determined although a preliminary description of the thermodynamics of binding of these inhibitors to both basal and "activated" forms have recently been reported.[19,20]

MEK1, similar to other protein kinases, is regulated by phosphorylation and thus exists in high and low activity states. These distinct states can adopt different conformations, which, in turn, can interact with ligands and inhibitors differently. The preferential binding of inhibitors to low versus high activity states would also determine the mode of action of a compound. For example, a compound that binds the unphosphorylated MEK1 preferentially over phosphorylated MEK1 could function by impacting RAF1-mediated MEK1 phosphorylation over MEK1-mediated ERK2 phosphorylation. There is conflicting data in the literature regarding the mode of action of the reported allosteric MEK1 inhibitors. In one study, U0126 and PD184352 inhibited RAF1-mediated MEK1 phosphor-

Received: April 11, 2011
Revised: July 27, 2011
Published: July 27, 2011

ylation rather than inhibiting MEK1-mediated ERK1 phosphorylation.[21] The authors also demonstrated that the inhibition of RAF1-mediated MEK1 activation required MEK1 and was thus due to direct binding of the inhibitors to MEK1. Another independent study corroborated these observations, wherein PD98059 did not inhibit phosphorylated MEK1 enzymatic activity but instead appeared to prevent RAF-mediated phosphorylation of wild-type MEK1.[22] These reports therefore suggested that the allosteric MEK1 compounds preferentially bound the nonphosphorylated form of MEK1. However, in a subsequent report, PD98059 and U0126 were shown to preferentially inhibit a recombinant, constitutively activated version of MEK1, ΔN3-S218E/S222D versus the wild-type enzyme.[23] In the most recent studies by Smith et al., the authors showed that the full-length wild-type MEK1 in unphosphorylated and RAF1-activated forms had comparable binding affinity for the two allosteric inhibitors: U0126 and PD0325901.[19] Thus, with the amount of conflicting data, the mechanism of MEK1 inhibition by the non-ATP-competitive compounds remains largely controversial.

Smith et al. generated phosphorylated MEK1 by coexpression with RAF1 in insect cells,[24] hereon referred to as pMEK1$^{in\ situ}$. A phosphatase inhibitor (okadaic acid) was also added during the harvesting and extraction phase in order to maximize the yield of the phosphorylated MEK1. In the present follow-up study, we report an alternative preparative method for activating MEK1 through *in vitro* phosphorylation by RAF1. The phosphorylated MEK1 produced by *in vitro* RAF1 activation is hereon referred to as pMEK1$^{in\ vitro}$. We demonstrate that there were marked differences in the phosphorylation states and occupancy and catalytic activity of the two activated forms of MEK1: pMEK1$^{in\ situ}$ and MEK1$^{in\ vitro}$. The thermodynamics of binding of allosteric inhibitors to pMEK1$^{in\ vitro}$ were investigated and contrasted with that of pMEK1$^{in\ situ}$. Contrary to previous findings, our results showed that the U0126 and PD0325901 preferentially bound the npMEK1 form over the pMEK1$^{in\ vitro}$ form, indicating the two protein forms have distinct inhibitor sites. The nucleotide-bound forms of npMEK1 and pMEK1$^{in\ vitro}$ showed higher affinity for PD0325901 compound and not the U0126 compound based on thermal-shift assay analyses. Finally, the work described here provides a sound basis for future structural studies of inhibitors bound to the activated form of MEK1.

EXPERIMENTAL PROCEDURES

Materials. PD0325901 was synthesized at Schering-Plough Research Institute (now Merck Research Laboratories). Its identity was confirmed by NMR and LC-MS. U0126 was obtained from Calbiochem. Staurosporine, K252a, and nucleotides used in this study were obtained from Sigma. All chemicals were obtained from Sigma (St. Louis, MO) unless otherwise specified. The purified pMEK1$^{in\ situ}$ and the full-length MEK1 plasmid were a generous gift from Dr. Catherine K. Smith from Merck Research Laboratories. GST-c-RAF1 (Y340D-Y341D) was purchased from Invitrogen Corp (San Diego, CA) or Millipore (Carrigtwohill, Ireland).

MEK1 Expression and Purification. The full-length construct used in this study was identical to the construct described by Smith et al.[24] The expression and purification of the nonphosphorylated full-length MEK1 was carried out as previously described. Briefly, MEK1 was expressed in High-Five (Invitrogen Corp, San Diego, CA) insect cells and purified to homogeneity using anion exchange and Ni-NTA chromatography followed by gel filtration. The protein was stored at −80 °C in the gel-filtration buffer (20 mM HEPES pH 7.5, 300 mM NaCl, 10% glycerol, and 1 mM DTT). The RAF1-mediated MEK1 activation was carried out in an *in vitro* setting as follows. The purified npMEK1 was incubated with GST-c-RAF1 (Y340D-Y341D) in 1:100 molar ratio in the storage buffer supplemented with 1 mM ATP and 5 mM $MgCl_2$ for 1 h at room temperature followed by an overnight incubation at 4 °C with gentle tumbling. The MEK1 phosphorylation after overnight incubation was deemed saturating based on Western blot results using antiphospho MEK1 specific antibodies (data not shown). To remove the GST-c-RAF1 (Y340D-Y341D) from the reaction mixture, the sample was loaded onto a GST Sepharose (GE Healthcare, Piscataway, NJ). The flow-through from the GST Sepharose column was concentrated and loaded onto a S200 gel-filtration column (GE Healthcare, Piscataway, NJ) to separate residual nucleotides and $MgCl_2$ from the activated pMEK1.

ERK2 Phosphorylation Assay. The ERK2 phosphorylation rates (nmol of Pi incorporated/min) were measured for each preparation of MEK1 (npMEK1, pMEK1$^{in\ situ}$, and pMEK1$^{in\ vitro}$) under the defined conditions: 0.1 M sodium MOPS, pH 7.2, 10 mM $MgCl_2$, 0.2 mg/mL BSA, 1 mM DTT, 2 μM ATP (0.5K_m), 1 μM ERK2 (~4K_m), and 5 nM MEK1. The activity was initiated by the addition of 5 × ATP stock containing <0.1% [γ^{32}P] ATP. The kinase activity was quenched at selected time points by spotting aliquots of the assay mixture on P-81 phosphocellulose paper and immersion in 1% phosphoric acid. After 3 washes in 1% phosphoric acid, the P-81 paper was dried in acetone, placed in 20 mL LSC vials containing liquid scintillation cocktail, and counted in a β counter ^{32}P channel. The specific activity values (nmol of Pi incorporated/(min mg of MEK1)) were calculated by dividing each rate value by the mg of MEK1/L.

LC-MS Analysis. The protein was reduced by incubating with 10 mM DTT at 56 °C for 30 min. After cooling to room temperature, the sample was alkylated by 20 mM indoacetamide under dark at room temperature for 45 min. 1 M NH_4HCO_3 was diluted in the sample to make its final concentration to 50 mM. Sequencing grade trypsin (Promega, Madison, WI) was added at 1: 25 w/w to each sample for digestion and incubated at 37 °C for 14 h. For chymotrypsin digestion, enzyme (Roche, Indianapolis, IN) was added at 1:20 w/w ratio and incubated overnight at 25 °C. Digested samples were diluted before LC-MS analysis. Peptide mixtures were analyzed by nano LC-ESI MS/MS in data-dependent acquisition mode. Chromatography was performed using a nano 2D HPLC system (Ekisigent, Dublin, CA). The peptide samples were loaded by autosampler onto a C18 trap column (0.3 × 50 mm, Dionex, Sunnyvale, CA) with 5% solvent B (0.1% formic acid in 97% ACN) at 10 μL/min for 5 min. Then the peptides were separated by a nanobore picofrit column (C18, 75 μm × 150 mm, 100 Å, New Objective, Woburn, MA) using a 45 min gradient from 5% to 95% B at a flow rate of 350 nL/min, where solvent A was 0.1% formic acid with 3% ACN in HPLC grade water. Eluted sample was analyzed by LTQ-Orbitrap mass spectrometer (Thermo, Waltham, MA) equipped with a nanoelectrospray ion source (Picoview PV500, New Objective, Woburn, MA). The spray voltage was set at 1.9 kV with sheath gas turned off. The data-dependent acquisition mode was performed by acquiring one full scan mass spectrum in FT mode (Rs = 30 000), followed by MS/MS of the top five most intensive peptide peaks (2+ and 3+ ions) in

ion trap with dynamic exclusion enabled. The m/z range is 300−1900.

Western Blot Analysis. npMEK1, pMEK1$^{in\ situ}$, and pMEK1$^{in\ vitro}$ were resolved on 4−12% Bis-Tris NuPAGE gel using MES running buffer and transferred to PVDF membrane. The membrane was blocked with 5% nonfat dried milk protein in TBS/T buffer (20 mM Tris pH 7.5, 500 mM NaCl, 0.1% polyoxyethysorbitan monolaurate) and then incubated overnight 4 °C with either anti-MEK1, antiphospho MEK1 (pSer218/pSer222), antiphospho MEK1 (pSer298), or antiphospho-MEK1 (pThr292) antibodies (Millipore, Carrigtwohill, Ireland) diluted 1:1000 in TBS/T containing 2% nonfat dried milk protein. After incubation with primary antibodies, the membranes were washed three times for 10 min each with TBS/T buffer at room temperature and then incubated for 2 h at room temperature with a 1:3000 dilution of HRP-linked anti-rabbit IgG (Millipore, Carrigtwohill, Ireland) in TBS/T containing 2% nonfat dried milk protein. The membranes were washed as before, and specific bands were developed using the ECL-Plus Western blotting detection system.

Temperature-Dependent Fluorescence (TdF). The setup for fluorescence-based thermal shift assays has been described previously.[25−27] For MEK1, the TdF experiments were conducted with and without 1 mM AMP-PnP, the concentration which was deemed as saturating under the TdF setup, for evaluating the binding of U0126, PD0325901, K252a, and staurosporine to different MEK1 preparations. The instrument used for these studies was Chromo4 RT-PCR instrument (Bio-Rad Laboratories Inc., Hercules, CA) equipped with a Peltier element block, four LEDs for illumination, and four filtered photodiodes for detection. The Opticon monitor 2 software interface was used for experimental setup and data acquisition. For individual melting experiments, the temperature was ramped from 20 to 80 °C in 0.2 °C increments. The temperature was allowed to stabilize with a 200 ms delay before reading. The fluorescence signals were acquired with excitation and emission wavelengths centered at 490 and 560 nm, respectively. A customized program using a nonlinear least-squares method based on the generalized reduced gradient (GRG2) algorithm was used to fit the protein unfolding model published in Matulis et al.[25] The fluorescence intensities of Sypro orange dye (Invitrogen Corp, San Diego, CA) are generally linearly dependent on temperature. The following parameters were floated during the fitting process: Y intercepts for the intensity of Sypro orange in both the native and denatured protein (Y_n and Y_d), their slopes (M_n and M_d), the midpoint of melting (T_m) and enthalpy at T_m (ΔH_m). The heat capacity at T_m (ΔC_p) was kept constant.

The relationship between ligand binding and protein stability as detected by changes in the midpoint of unfolding (T_m) has been well-documented, and K_d values can be calculated from the ΔT_m.[25,26] Equation 1 was used to calculate K_d values for inhibitor binding to MEK1 proteins. The ligand binding constant ($K_L(T)$) can be calculated at any temperature (T) by the following equation:

$$K_L(T) = K_L(T_m) \exp\left\{\left(\frac{-\Delta H_L(T)}{R}\right)\left(\frac{1}{T} - \frac{1}{T_m}\right) + \left(\frac{\Delta C_{pL}}{R}\right)\left[\ln\frac{T}{T_m} + 1 - \frac{T}{T_m}\right]\right\} \quad (1)$$

where T_m is the midpoint of unfolding in the presence of ligand, ΔH_L is the enthalpy of binding, ΔC_{pL} is the ligand binding heat capacity, and K_L (T_m) is the ligand binding constant at T_m. If estimates for both ΔH_L and ΔC_{pL} are available, then the ligand binding constant, K_L (T), can be calculated at any temperature T (assuming that the heat capacity term is temperature independent). K_L (T_m) can be calculated by the following equation:

$$K_L(T_m) = \{\exp\{-(\Delta H_u(T_0)/R)(1/T_m - 1/T_0) + (\Delta C_{pu}/R)[\ln(T_m/T_0) + (T_0/T_m) - 1]\} - 1\}/[L_{T_m}] \quad (2)$$

where T_0 is the midpoint of unfolding for the unliganded protein, T_m is the midpoint of unfolding in the presence of ligand, ΔH_u is the enthalpy of protein unfolding, ΔC_{pu} is the heat capacity associated with protein unfolding, and $[L_{T_m}]$ is the free concentration of ligand at T_m. Unless otherwise specified, ΔH_L values were assumed to be −7 kcal/mol and ΔC_{pL} was set to zero for TdF-determined $K_L(T)$.[28]

AS-MS Setup for K_d Measurements. The general size-exclusion chromatography (SEC)-based AS-MS hardware configuration used in this study has been described previously.[29−31] Briefly, this system uses continuous SEC to isolate protein−ligand complexes from unbound ligand. Samples containing a target protein, protein−ligand complexes, and unbound ligand were injected onto an SEC column, where the complexes were separated from nonbinding component by a rapid SEC step. SEC was performed at 4 °C using buffered saline, typically 50 mM, pH 7.5 phosphate buffer containing 150 mM NaCl. The eluant from the SEC column was passed through a UV detector (Agilent G1314A using a G1313 microflow cell) where the band containing the protein−ligand complex was identified by its native UV absorbance at 230 nm. After a pause to allow the band to leave the first detector and enter a valving arrangement, the protein−ligand complex peak was automatically transferred to a reversed-phase chromatography (RPC) column (Higgins Targa-C_{18}, 0.5 mm i.d. × 50 mm length, Higgins Analytical Inc.). Ligands were dissociated from the complex and trapped at the head of the RPC column, where they were desalted and eluted into the mass spectrometer using a gradient of 0−95% acetonitrile (0.1% formic acid) in water (0.1% formic acid) over 5 min using an Agilent capillary binary pump (G1376A) for eluant delivery at 20 μL/min. To promote dissociation of ligands from the complex, the RPC column was maintained at 60 °C using an Agilent G1316A column compartment. In this study, MS analysis was performed using a Waters LCT "Classic" high-resolution time-of-flight mass spectrometer (Manchester, U.K.) with positive-mode ionization occurring from a standard nebulized electrospray ionization (ESI) source with the capillary at 3.5 kV, a desolvation temperature of 180 °C, a source temperature of 100 °C, and 30 V "cone" and 3 V extraction lens settings. The lagging free

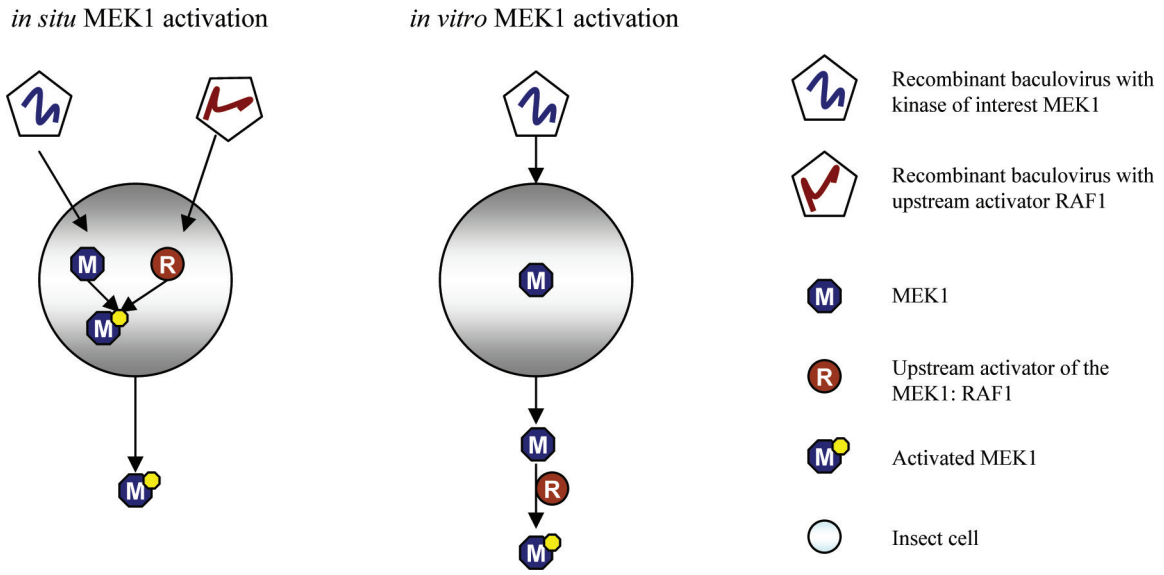

Figure 1. Overview of the two MEK1 activation strategies employed to generate pMEK1. In the *in situ* activation process, the MEK1 and RAF1 containing recombinant baculoviral stocks are used to coinfect the insect cells. The coexpression of the two proteins results in phosphorylation of MEK1 catalyzed by RAF1. The lysis of insect cells and subsequent purification yields phosphorylated MEK1, pMEK1$^{in\ situ}$. Alternatively, in the *in vitro* activation strategy, only MEK1 in expressed in insect cells and purified to homogeneity. Once purified, the protein is activated by incubation with purified RAF1 *in vitro*. The final *in vitro* activated MEK1 is called pMEK1$^{in\ vitro}$.

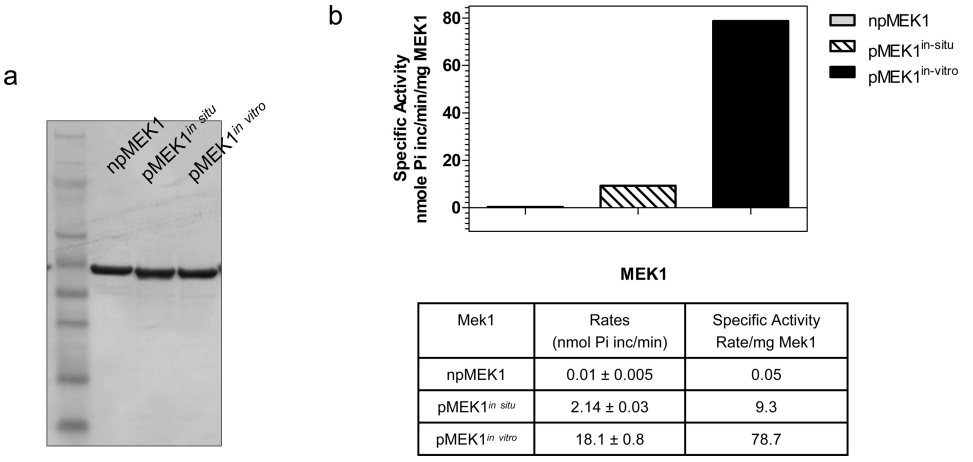

Mek1	Rates (nmol Pi inc/min)	Specific Activity Rate/mg Mek1
npMEK1	0.01 ± 0.005	0.05
pMEK1$^{in\ situ}$	2.14 ± 0.03	9.3
pMEK1$^{in\ vitro}$	18.1 ± 0.8	78.7

Figure 2. Samples of purified npMEK1, pMEK1$^{in\ situ}$, and pMEK1$^{in\ vitro}$ were subjected to Nu-PAGE (4−12%) in MES running buffer and stained with Coomassie blue R-250 for purity comparison. The specific activity and phosphate incorporation rates are depicted in the figure and table on the right. Specific activity was determined using the filter binding format. Specific activity = nmol incorporated/(time (min) × mg protein in reaction) over linear phase of each reaction. The phosphate (nmol) incorporated into ERK2 was determined using nmol incorporated = (counts incorporated × nmol ATP available)/(total counts available).

ligand peak from SEC was subsequently recovered by redirecting the mobile phase path through SEC and RPC columns. Capture of the free ligand onto RPC and MS analysis was as described for the protein−ligand complex. Ion current detection of ligand at expected mass was used to quantify the bound and free forms observed in the AS-MS setup. Prior calibration was performed by injecting varying concentrations of ligands in the binding buffer (20 mM HEPES pH 7.5, 300 mM NaCl, 10% glycerol, and 1 mM DTT). The experimentally determined bound and free fractions were fitted to the Scatchard equation for determination of binding constant (K_d).

Isothermal Titration Calorimetry (ITC). Purified pMEK1$^{in\ vitro}$ was dialyzed extensively against 50 mM HEPES at pH 7.4, 300 mM NaCl, 1 mM $MgCl_2$, and 1 mM DTT. The protein was diluted at the appropriate concentration with dialysate buffer immediately prior to the experiment. PD0325901 was prepared in 100% DMSO and added such that the final solution contained 1% DMSO. For this titration, the DMSO was added to the protein solution at the same percentage. The binding of PD0325901 was assessed by injecting 200 μM PD0325901 into 20 μM MEK1 protein solution. ITC experiments were performed with a Microcal ITC_{200} titration calorimeter (Microcal Inc., North Hampton, MA). Protein and nucleotide solutions were centrifuged for 5−10 min at room temperature prior to loading the samples in the ITC cell and syringe. All titrations were carried out at 20 °C with a stirring speed of 350 rpm and a 180 s duration between each 3 μL injection. Parallel experiments were performed by injecting the nucleotide into the buffer or the buffer into the protein to determine heats of dilution. The heats of dilution were negligible in all cases and

dx.doi.org/10.1021/bi200542r | *Biochemistry* 2011, 50, 7964−7976

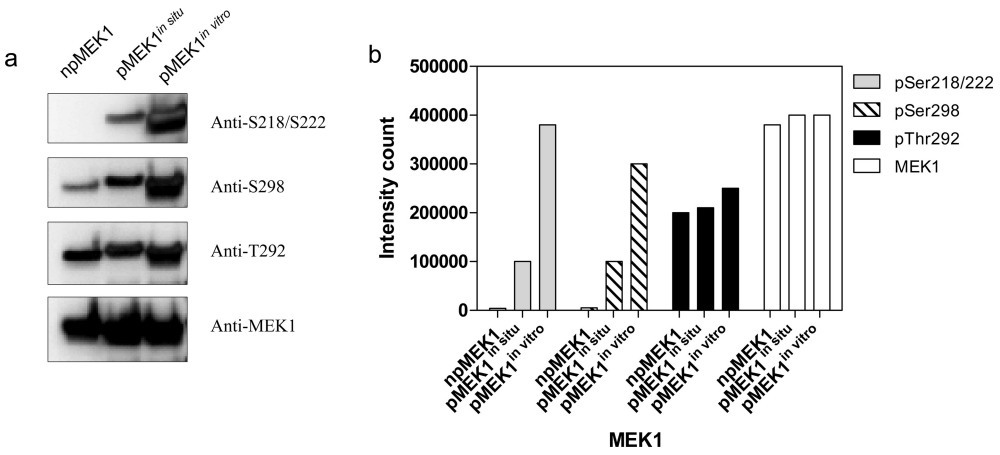

Figure 3. Western blot analyses of MEK1 preparations. Samples of purified npMEK1, pMEK1$^{in\ situ}$, and pMEK1$^{in\ vitro}$ were subjected to Nu-PAGE (4−12%) in MES running buffer and stained with Coomassie blue R-250. Proteins were transferred to nitrocellulose and blotted using anti-MEK1, antiphospho MEK1 (pSer217/pSer221), antiphospho MEK1 (pSer298), or antiphospho-MEK1 (pThr292) antibodies. The right panel depicts quantitative densitometric analyses of the Western blotting data.

were subtracted from their respective titrations prior to data analysis.

The values for N (stoichiometry), K_a (association constant), and ΔH (enthalpy change) were obtained by nonlinear least-squares fitting of experimental data using a single-site-binding model of the Origin software package (version 5.0) provided with the instrument. The free energy of binding (ΔG) and entropy change (ΔS) were obtained using the following equations:

$$\Delta G = -RT \ln K_a \quad (3)$$

$$\Delta G = \Delta H - T\Delta S \quad (4)$$

The affinity of the inhibitor to protein is given as the dissociation constant ($K_d = 1/K_a$). For accurate parameter determination, three titrations were performed. Titration data were analyzed independently, and derived values obtained were averaged.

RESULTS

Purification and Activation of Full-Length MEK1 Protein from Insect Cells. The differences in the *in vitro* and the *in situ* activation strategies are outlined in Figure 1. In the *in vitro* activation process, several disadvantages of the *in situ* activation process were circumvented. The *in vitro* activation process eliminated the need for maintenance of active baculoviral stocks of cRAF1, since purified recombinant RAF1 was utilized for the activation purposes. This was particularly useful in light of the availability of pure activated cRAF1 protein from commercial vendors such as Invitrogen and Millipore. The *in vitro* activation process also allowed for a controlled activation reaction, wherein the molar ratios of RAF1:MEK1 could be easily varied based on the measured enzymatic activity of RAF1 protein. Lastly, since homogeneously purified MEK1 was used as a substrate for RAF1 protein for activation, the need for adding okadaic acid (an expensive reagent) to expression media and buffers was eliminated.

The high level of expression of the protein in High-Five cells that was reported by Smith et al. was reproduced in our laboratory. npMEK1 was purified using the three-step purification protocol consisting of anion exchange, Ni-NTA, and gel-filtration chromatography, respectively. The purity of npMEK1 protein is represented in Figure 2a (lane 2). The purified npMEK1 was incubated with GST-cRAF1 (Y340D + Y341D) in the presence of saturating amounts of ATP and $MgCl_2$. The reaction was allowed to continue overnight at 4 °C for completion. The GST-cRAF1 was purified from pMEK1$^{in\ vitro}$ using GST-sepharose affinity chromatography. The activated pMEK1$^{in\ vitro}$ was then subjected to gel-filtration chromatography to remove residual nucleotides and additives from the activation reaction. The pMEK1$^{in\ vitro}$ form of the protein was >90% pure (Figure 2a) and existed as a monomer in solution based on the elution profile of the protein from gel-filtration chromatography (data not shown).

Characterization of Activated pMEK1$^{in\ vitro}$. MEK1 enzymatic activity was measured based on direct phosphorylation of its natural substrate, ERK2 protein, and the specific activity is reported in Figure 2b. Nonphosphorylated MEK1, npMEK1, showed low but detectable activity in the radioactive filter binding ERK2 phosphorylation assay (specific activity 0.05 U/mg). The *in situ*-activated MEK1 exhibited 186-fold higher specific activity (9.3 U/mg) than the npMEK1 form, while the *in vitro*-activated MEK1 (78.7 U/mg) showed 1574-fold increase in the specific activity compared to the npMEK1. Most significantly, the pMEK1$^{in\ vitro}$ showed 8.4-fold higher specific activity than its pMEK1$^{in\ situ}$ counterpart (78.7 U/mg vs 9.3 U/mg). These results demonstrated marked differences in the catalytic efficiency of the two different RAF1-activated MEK1 preparations: pMEK1$^{in\ situ}$ and pMEK1$^{in\ vitro}$.

To probe the source of the difference in the catalytic activities of pMEK1$^{in\ situ}$ and pMEK1$^{in\ vitro}$, we investigated the phosphorylation patterns of the two proteins and compared them to npMEK1. Western blot analyses using antiphospho MEK1 antibodies were performed to investigate the phosphorylation state of npMEK1, pMEK1$^{in\ situ}$, and pMEK1$^{in\ vitro}$. As shown in Figure 3, the three MEK1 preparations showed differences in phosphorylation levels at the known T-loop sites, Ser218 and Ser222. npMEK1 showed no significant phosphorylation at Ser 218/222. pMEK1$^{in\ situ}$ showed >4-fold lower phosphorylation signal at the T-loop sites compared to pMEK1$^{in\ vitro}$ (Figure 3). A similar pattern was seen for Ser298 site. The level of phosphorylation at Ser298 was npMEK1 < pMEK1$^{in\ situ}$ < pMEK1$^{in\ vitro}$. The phosphorylation of

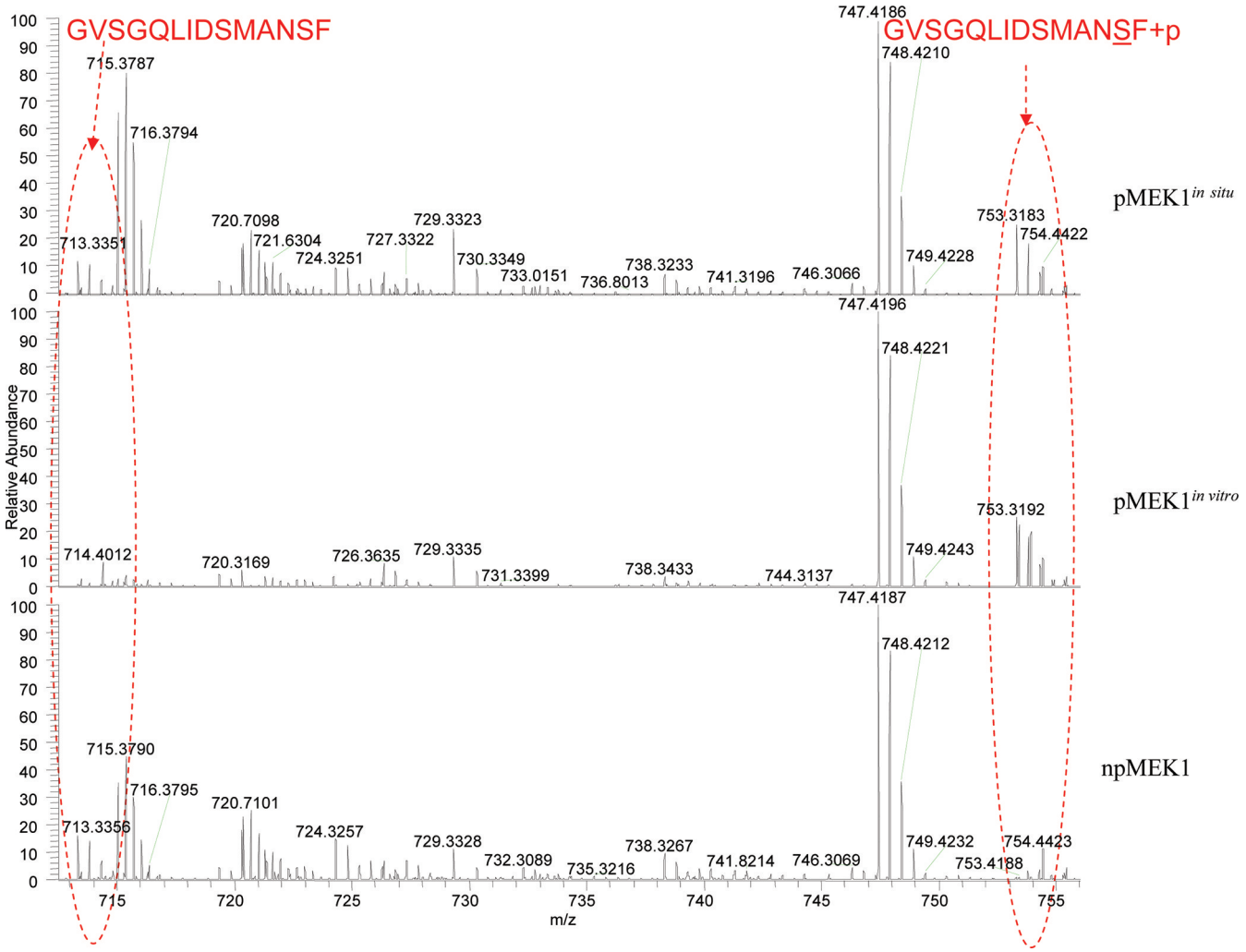

Figure 4. Mass spectrum (Orbi/IT) of peptide G234-F247, GVSGQLIDSMANSF in (top panel) pMEK1$^{in\text{-}situ}$, (middle panel) pMEK1$^{in\text{-}vitro}$, and (bottom panel) npMEK1. Theoretical mass of G234-F247 is 1425.6679 (MH+). It is observed in sample pMEK1$^{in\text{-}situ}$ and npMEK1 with mass shift of 3.8 ppm and 3.2 ppm. Theoretical mass with one phosphorylation is 1505.6342 (MH+). Phosphorylated form is observed in sample pMEK1$^{in\text{-}situ}$ and pMEK1$^{in\text{-}vitro}$ with mass shift of 3.6 ppm and 2.4 ppm.

Thr292 site in the three MEK1 preparations was comparable. Anti-MEK1 antibody was used to identify both phosphorylated and nonphosphorylated MEK1 proteins for loading control (Figure 3). To further investigate the T-loop phosphorylation state of the MEK1 preparations, we employed LC-MS analyses. Phosphopeptide mapping indicated that peptide harboring the T-loop Ser218 and S222 (GVSGQLIDSMANSF) was completely unphosphorylated in npMEK1 (Figure 4), fully phosphorylated on pMEK1$^{in\ vitro}$, and existed in both unphosphorylated and phosphorylated forms in pMEK$^{in\ situ}$, indicating that the pMEK1$^{in\ situ}$ protein phosphorylation on T-loop is not stoichiometric. The phosphopeptide mapping analyses identified phosphorylation at Ser222 and not Ser218 in the pMEK1 preparations (Figure 5). The level of Ser222 phosphorylation on pMEK1$^{in\ situ}$ and pMEK1$^{in\ vitro}$ was calculated to be 30% and >95%, respectively based on MS signal intensities. Taken together, these results indicated that the pMEK1$^{in\ vitro}$ protein was fully phosphorylated on the T-loop. The higher level of T-loop phosphorylation could have contributed to its high specific activity in pMEK1$^{in\ vitro}$ compared to its pMEK$^{in\ situ}$ counterpart.

Thermodynamics of Inhibitor Binding to MEK1$^{in\ vitro}$.

Smith et al. demonstrated that npMEK1, although enzymatically inactive, was capable of binding known MEK1 inhibitors with an affinity that was comparable with the activated pMEK$^{in\ situ}$.[19] The differences in the phosphorylation levels and specific activity of pMEK1$^{in\ vitro}$ and pMEK$^{in\ situ}$ compelled us to retest the prior conclusions regarding effects of MEK1 phosphorylation on binding of allosteric inhibitors U0126 and PD0325901. Thermal denaturation studies on the three forms of MEK1 were performed and contrasted against previously published results. Figure 6a–c shows that all three forms of the MEK1 protein showed unfolding in response to increasing temperature in a sigmoidal fashion as expected for a native-like protein that unfolds in a cooperative manner. The midpoint of the unfolding transition (T_m) was 50 ± 0.2 °C for npMEK1 and 50 ± 0.1 °C for pMEK$^{in\ situ}$, while pMEK1$^{in\ vitro}$ T_m was 48.6 ± 0.1 °C. Based on these results, all three proteins appear to be stably folded in solution. The binding of known inhibitors to the three forms of the protein was subsequently tested in the thermal shift assay. The additional stabilizing interactions created between the ligand and the protein allows a protein to become more resistant to thermal unfolding relative to

dx.doi.org/10.1021/bi200542r | Biochemistry 2011, 50, 7964–7976

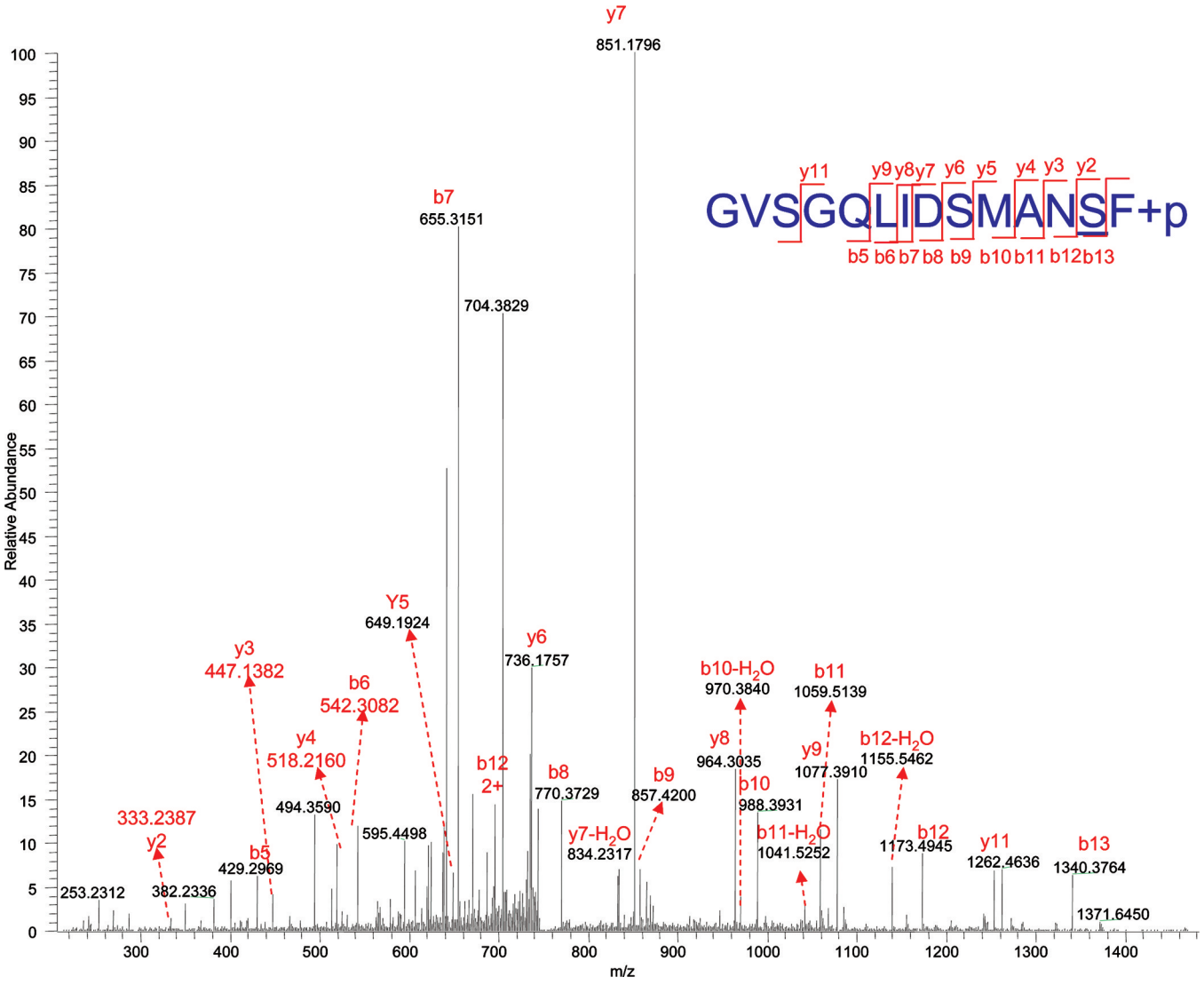

Figure 5. MS/MS spectrum (Orbi/IT) of peptide G234-F247, GVSGQLIDSMANSF, S222 is phosphorylated.

unliganded apo protein. The changes in the protein T_m in the presence of the inhibitor compared to apo protein T_m correlate with the affinity of the protein for the ligand.

The inhibitors used in this study can be divided into two categories: ATP site inhibitors (K252a and staurosporine) and allosteric inhibitors (U0126 and PD0325901). In the presence of K252a, staurosporine, U0126, and PD0325901, npMEK1 showed ΔT_m of 10.5 ± 0.28, 9.2 ± 0.3, 4.7 ± 0.3, and 2.5 ± 0.25 °C, which corresponded to calculated TdF K_ds of 0.015, 0.037, 0.7, and 4 μM, respectively (Figure 6a and Table 1). In the presence of the inhibitors under identical conditions, the pMEK$^{in\ situ}$ protein showed results (ΔT_m of 10.5 ± 0.3 °C (K252a), 9.4 ± 0.2 °C (staurosporine), 4.6 ± 0.17 °C (U0126), and 2.6 ± 0.15 °C (PD0325901)) that were comparable to npMEK1 (Figure 6b and Table 1). These ΔT_m results for npMEK1 and pMEK$^{in\ situ}$ are largely consistent with those observed by Smith et al. with an alternative thermal shift assay using circular dichroism as readout for protein unfolding.[19] On the basis of these results, the authors reported that there was no significant difference in the binding of inhibitors between inactive and RAF1-activated MEK1. In our experiments, however, we observed significant differences between the inhibitor binding affinities of pMEK1$^{in\ vitro}$ and npMEK1 and pMEK$^{in\ situ}$. In contrast to npMEK1 and pMEK$^{in\ situ}$, pMEK1$^{in\ vitro}$ protein showed significantly higher ΔT_m values for ATP site inhibitors (ΔT_m = 13.7 ± 0.3 °C for K252a, and ΔT_m = 11.1 ± 0.2 °C for staurosporine) and lower ΔT_m values for allosteric site inhibitors (ΔT_m = 1.8 ± 0.17 °C for U0126, and ΔT_m = 0.6 ± 0.15 °C for PD0325901) compared to npMEK1 (Figure 6a,c and Table 1). The differences in the ΔT_m values translate into 10- and 8-fold lower affinity for U0126 and PD0325901 by pMEK1$^{in\ vitro}$ compared to npMEK1 (based on eq 2). These inhibitor binding studies indicate the following: (1) both npMEK1 and pMEK$^{in\ situ}$ show comparable affinity for all inhibitors tested; (2) pMEK1$^{in\ vitro}$ bound ATP-competitive inhibitors K252a and staurosporine with higher affinity than its nonphosphorylated counterpart, npMEK1; (3) in its fully phosphorylated form, pMEK1$^{in\ vitro}$ binds allosteric inhibitors U0126 and PD0325901 with lower affinity than npMEK1.

To test whether the findings from thermal shift assay were consistent across different binding assay formats, we applied affinity selection mass spectrometry (AS-MS) and isothermal titration calorimetry (ITC) for studying MEK1−inhibitor interaction. Figure 7 shows the AS-MS results for binding of U0126 and PD0325901 to npMEK1 and pMEK1$^{in\ vitro}$. In the AS-MS system, U0126 and PD0325901 were recovered in the

dx.doi.org/10.1021/bi200542r | Biochemistry 2011, 50, 7964−7976

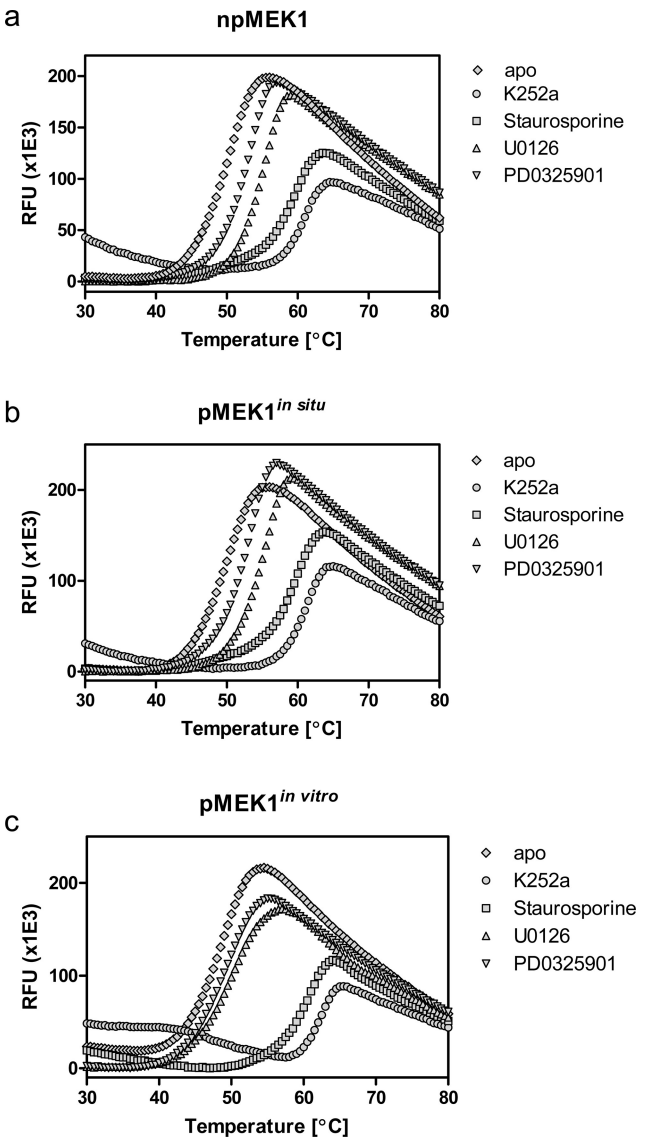

Figure 6. TdF analyses of U0126, PD0325901, staurosporine, and K252a binding to npMEK1 (a), pMEK1$^{in\ situ}$ (b), and pMEK1$^{in\ vitro}$ (c). (a) Thermal denaturation curves for npMEK1 alone (◆), + K252a (●), + staurosporine (■), + U0126 (▲), + PD0325901 (▼). (b) Thermal denaturation curves for pMEK1$^{in\ situ}$ alone (◆), + K252a (●), + staurosporine (■), + U0126 (▲), + PD0325901 (▼). (c) Thermal denaturation curves for pMEK1$^{in\ vitro}$ alone (◆), + K252a (●), + staurosporine (■), + U0126 (▲), + PD0325901 (▼).

npMEK1 fraction of the SEC, which is indicative of ligand binding. However, in contrast to npMEK1, lower amounts of ligands were recovered in the protein-bound portion of SEC for pMEK1$^{in\ vitro}$, implying weaker affinities below the detection limit of the instrumentation setup. The AS-MS system was calibrated with known concentrations of ligands, and saturation binding experiment was performed for both npMEK1 and pMEK1$^{in\ vitro}$. npMEK1 bound U0126 and PD0325901 with AS-MS K_d of 2 ± 0.5 and 5 ± 1 μM. Low MS signal intensities in the protein-bound portion of pMEK1$^{in\ vitro}$ precluded K_d determination, and therefore the K_d values were set at >10 μM, which was calculated to be the detection limit of the experimental setup. The differences in the binding affinities of npMEK1 and pMEK1$^{in\ vitro}$ for the allosteric inhibitors seen in the AS-MS setup were consistent with the data from thermal shift assay.

On the basis of the TdF and AS-MS results, ITC binding studies were performed with pMEK1$^{in\ vitro}$ and PD0325901 to obtain a more complete thermodynamic analysis of inhibitor binding to pMEK1$^{in\ vitro}$. Panels a and b of Figure 8 show representative calorimetric titration of pMEK1$^{in\ vitro}$ with PD0325901. The exothermic evolution of heat upon inhibitor injections shown in the upper panel illustrates saturable inhibitor binding by the protein. An analysis of the enthalpy change versus molar ratio of PD0325901 (lower panel) revealed an apparent K_d = 5 ± 0.2 μM for PD0325901. The measured ΔH_L was −5.8 ± 0.7 kcal/mol, and the calculated $-T\Delta S$ was −1.3 kcal/mol. On the basis of these results, it appears that binding of PD0325901 to full-activated pMEK1$^{in\ vitro}$ is enthalpically driven albeit entropically favorable. The poor solubility of U0126 precluded accurate determination of its affinity to pMEK1$^{in\ vitro}$. The ITC experiments were performed under identical conditions as previously reported for npMEK1.[19] Comparison of the K_d values obtained for both npMEK1 and pMEK1$^{in\ vitro}$ indicates that the loss of affinity for PD0325901 in pMEK1$^{in\ vitro}$ is due to differences in ΔH_L rather than ΔS (Figure 8), implying loss of key hydrogen-bonding interactions within the context of pMEK1$^{in\ vitro}$·PD0325901 complex compared to npMEK1·PD0325901. The differences in binding of allosteric inhibitors between two MEK1 preparations are thus consistently observed across different assay formats.

Thermodynamics of Inhibitor Binding by MEK1$^{in\ vitro}$·AMP-PnP Complex. Previous studies have shown that the presence of nucleotide increases the affinity of PD0325901 in npMEK1 and pMEK1$^{in\ situ}$. We sought to investigate whether that was true for pMEK1$^{in\ vitro}$ using thermal shift assay. The TdF binding studies between PD0325901 and npMEK1·AMP-PnP complex gave a larger shift in the T_m (ΔT_m = 10.4 ± 0.3 °C) compared to that given by inhibitor binding to apo npMEK1 (ΔT_m = 2.5 ± 0.25 °C) (Tables 1 and 2). Thus, the binding of nucleotides increases the affinity of PD0325901 for npMEK1 by 444-fold ($\Delta\Delta T_m$ = 7.9 °C). The pMEK1$^{in\ vitro}$ protein demonstrated 135-fold increase in affinity for PD0325901 in the presence of nucleotide. The ΔT_m in the presence of 25 μM PD0325901 for pMEK1$^{in\ vitro}$ protein and pMEK1$^{in\ vitro}$·AMP-PnP protein complex were 0.6 ± 0.15 and 7.5 ± 0.2 °C, respectively (Tables 1 and 2). Although the inhibitor binding affinity in the presence of nucleotide increased substantially for pMEK1$^{in\ vitro}$, the activated nucleotide-bound protein showed 22-fold lower affinity for PD0325901 than its nucleotide-bound npMEK1 counterpart (TdF K_d of 0.2 μM (pMEK1$^{in\ vitro}$·AMP-PnP) versus 0.009 μM (npMEK1·AMP-PnP)). The TdF-based binding of U0126 was also measured for npMEK1·AMP-PnP and pMEK1$^{in\ vitro}$·AMP-PnP protein complexes. The ΔT_m for binding of U0126 to npMEK1 and npMEK1·AMP-PnP complex was comparable (4.7 ± 0.3 and 4.5 ± 0.2 °C, respectively (Tables 1 and 2)). Similarly, the binding of U0126 to pMEK1$^{in\ vitro}$ in its apo and nucleotide-bound form was comparable (ΔT_m 1.7 ± 0.15 °C and ΔT_m 1.8 ± 0.17 °C, respectively). These inhibitor binding studies in the presence of nucleotides indicate the following: (1) both npMEK1 and pMEK$^{in\ vitro}$ show higher affinity for PD0325901 in the presence of AMP-PnP compared to their apo counterparts; (2) npMEK1·AMP-PnP complex binds PD0325901 with higher affinity than pMEK1$^{in\ vitro}$·AMP-PnP; (3) although phosphorylation in MEK1 lowers the affinity for

dx.doi.org/10.1021/bi200542r | Biochemistry 2011, 50, 7964–7976

Table 1. TdF Analyses Performed and Analyzed As Described in the Experimental Procedures under Conditions Shown under "Ligands" Column[a]

	npMEK1			pMEK1$^{in\ situ}$			pMEK1$^{in\ vitro}$		
ligands	T_m (°C)	ΔT_m (°C)	TdFK_d[a] (μM)	T_m (°C)	ΔT_m (°C)	TdFK_d[a] (μM)	T_m (°C)	ΔT_m (°C)	TdFK_d[a] (μM)
apo	50 ± 0.2			50 ± 0.1			48.6 ± 0.1		
25 μM K252a	60.5 ± 0.08	10.5 ± 0.28	0.015	60.5 ± 0.2	10.5 ± 0.3	0.015	62.3 ± 0.2	13.7 ± 0.3	0.001
25 μM staurosporine	59.2 ± 0.1	9.2 ± 0.3	0.037	59.4 ± 0.1	9.4 ± 0.2	0.032	59.7 ± 0.1	11.1 ± 0.2	0.009
25 μM U0126	54.7 ± 0.1	4.7 ± 0.3	0.7	54.6 ± 0.07	4.6 ± 0.17	0.8	50.5 ± 0.07	1.8 ± 0.17	7
25 μM PD0325901	52.5 ± 0.05	2.5 ± 0.25	4	52.6 ± 0.05	2.6 ± 0.15	3.6	49.2 ± 0.05	0.6 ± 0.15	27

[a]Assuming ΔH_L for ligands = −7 kcal/mol. Standard error values from two to three experiments are as shown.

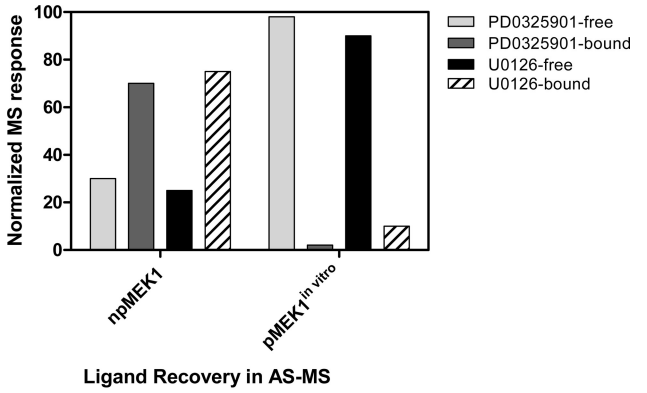

Ligands	AS-MS K_d (μM)	
	npMEK1	pMEK1$^{in\ vitro}$
U0126	2 ± 0.5	>10
PD0325901	5 ± 1	>20

Figure 7. AS-MS analyses of U0126 and PD0325901 binding to npMEK1 and pMEK1$^{in\ vitro}$. (Top figure) Binding of compounds U0126 and PD0325901 in the AS-MS system as determined by the recovery of the unbound and bound compound (from the dissociation of the protein−ligand complex from reverse phase chromatography) as described in the Experimental Procedures section. The data are shown as normalized mass spectrometry signal response under indicated conditions. (Bottom table) For the AS-MS K_d determination, compounds were added at variable concentrations MEK1 proteins in binding buffer containing 20 mM HEPES pH 7.5, 300 mM NaCl, 10% glycerol, and 1 mM DTT. The mixtures were incubated for 30 min at room temperature and then injected into the AS-MS system as described in the Experimental Procedures for determination of bound ligand (L_b) and free 4a (L_f). The results were fitted to the Scatchard equation $L_b = nP - K_d(L_b/L_f)$, where P is the total MEK1 concentration and n and K_d are the stoichiometry of binding and dissociation constant, respectively.

U0126, the binding of U0126 is not impacted by the presence of nucleotides for either form of the protein.

DISCUSSION

Approximately 30% of human tumors exhibit RAS-RAF-MEK-ERK2 dependence via increased signaling through that pathway. Thus, inhibition of this pathway is considered a promising approach for the treatment of cancer. Consistent with that hypothesis, several MEK1 inhibitors have entered clinical trials. The reported MEK1 inhibitors are structurally diverse and can either be ATP-competitive or ATP-non-competitive. While some data on the kinetics of inhibition of

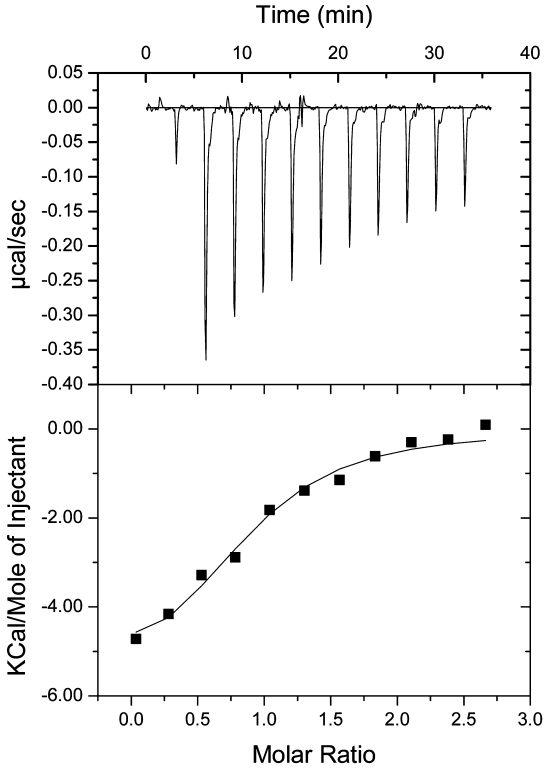

ITC	PD0325901		
	K_d (μM)	ΔH_L (kcal/mol)	$-T\Delta S$ (kcal/mol)
pMEK1$^{in\ situ}$	0.14[1]	-7.8[1]	-1.4[1]
pMEK $^{in\ vitro}$	5 ± 0.2	-5.8 ± 0.7	-1.3

[1]from Smith et al (2007)

Figure 8. ITC analyses of PD0325901 binding to pMEK1$^{in\ vitro}$. (Top figure) Raw isothermal titration calorimetry data (upper panels) and normalized ITC data for titrations plotted versus the molar ratio of titrant/protein (lower panels) demonstrating saturable exothermic evolution of heat upon sequential additions of PD0325901 to pMEK1$^{in\ vitro}$ in 50 mM HEPES at pH 7.4, 300 mM NaCl, 1 mM $MgCl_2$, and 1 mM DTT. Data analysis using Origin 5.0 software indicates that the binding data fit well to a single binding-site model. (Bottom table) Dissociation constants as well as changes in enthalpy and entropy values obtained from fitting of the ITC binding data in comparison with previously published results.

dx.doi.org/10.1021/bi200542r | Biochemistry 2011, 50, 7964–7976

Table 2. TdF Analyses Performed and Analyzed As Described in the Experimental Procedures under Conditions Shown under "Ligands" Column[a]

	npMEK1 + AMP-PnP			pMEK1$^{in\ vitro}$ + AMP-PnP		
ligands	T_m (°C)	ΔT_m (°C)	TdFK_d (μM)	T_m (°C)	ΔT_m (°C)	TdFK_d (μM)
no inhibitor	53.8 ± 0.1			51 ± 0.1		
25 μM U0126	58.3 ± 0.1	4.5 ± 0.2	0.7	52.7 ± 0.05	1.7 ± 0.15	9
25 μM PD0325901	64.2 ± 0.2	10.4 ± 0.3	0.009	58.5 ± 0.1	7.5 ± 0.2	0.2

[a]Assuming ΔH_L for ligands = −7 kcal/mol. Standard error values from two to three experiments are as shown.

two of the ATP noncompetitive inhibitors, U0126 and PD0325901, has been reported, there is much to be understood about the mechanism of inhibition by these compounds, especially in the context of different MEK1 states. In order to study the thermodynamics of binding of inhibitors to phosphorylated MEK1 and unphosphorylated MEK1, it is important to obtain stoichiometric T-loop phosphorylation for homogeneity in the phosphorylated MEK1 preparations. The existence of mixed phosphorylated and unphosphorylated species in MEK1 preparations can skew the K_d determination especially if the two states have different affinity for the inhibitors.

RAF1-mediated phosphorylation of MEK1 is a prerequisite for the activation of MEK1 enzymatic activity and subsequent ERK2 phosphorylation by MEK1. The method for producing both full-length inactive and "active" MEK1 from insect cells was previously described by Smith et al.[24] Our present study confirms these findings and further extends the characterization of the "active" MEK1 produced *in situ* by coexpression of cRAF1 and MEK1 in insect cells. pMEK1$^{in\ situ}$ was contrasted with MEK1 optimally phosphorylated *in vitro*, pMEK1$^{in\ vitro}$, using commercial sources of purified GST-cRAF1(Y340D +Y341D). The two preparations exhibited significant difference in the extent of T-loop phosphorylation and affinity profile for ATP site and allosteric inhibitors of MEK1.

All preparations of MEK1 derived from insect cells—npMEK1, pMEK$^{in\ situ}$, and pMEK1$^{in\ vitro}$—were phosphorylated at Thr292 and Ser298, albeit the latter was only detected in trace amount by Western blots in npMEK1. Ser298 is a known site for phosphorylation by p21-activated kinase (PAK) in humans, and an ortholog could potentially exist in insect cells. Phosphorylation at Ser298 does not intrinsically activate catalysis but facilitates docking of cRAF1 [32] for subsequent phosphorylation of the activation loop. More importantly, in the human system phosphorylation at Ser298 is required for docking of the ERK2, which upon activation could phosphorylate Thr292 through a feedback mechanism to inhibit further phosphorylation at Ser298 by PAK.[33,34] The existence of an orthologous RAF-MEK-ERK module operating in insect cells is unknown to us. However, we consistently detected strong phosphorylation at Thr292 by unidentified insect kinase(s), trace amounts at Ser298, and practically none at the T-loop of npMEK1 resulting in a catalytically inactive preparation. The pattern of MEK1 phosphorylation in insect cells in the absence of cRAF1 coexpression appears consistent with a feedback mechanism functioning similarly to the one described for the human system.

Coexpression of cRAF1 with MEK1 as described by Smith et al.[24] indeed allowed for the isolation of catalytically competent MEK1. Specific activity measured by phosphorylation assays increased by 186-fold, and the comparative Western blot analyses (Figure 3) demonstrated that pMEK1$^{in\ situ}$ was phosphorylated at the T-loop sites. Interestingly, phosphorylation at the T-loop site was also accompanied by increase in Ser298 phosphorylation. The available data indicate that coexpression of cRAF1 in insect cells increases the intracellular concentration of kinases capable of T-loop phosphorylation and overrode any inhibitory feedback mechanism exerted by phosphorylation at Thr292. The observed concomitant increase in phosphorylation at Ser298 could also be the result of direct phosphorylation of that residue by the *in situ* expressed cRAF1. The availability of pMEK1$^{in\ vitro}$ provided an outstanding opportunity for comparing the two phosphorylated preparations. It was very clear from the specific activity data of phosphorylation assays, and including the Western blots and mass spectrometry data (Figures 2−5), that pMEK$^{in\ situ}$ was only partially phosphorylated at the T-loop. According to our estimate, only 10−30% of pMEK$^{in\ situ}$ was actually activated by phosphorylation at the T-loop, whereas phosphorylation of pMEK1$^{in\ vitro}$ was essentially stoichiometric. The inefficiency of the *in situ* method was most likely the result of inadequate expression of intracellular cRAF1 (<0.1 mgs/L) compared to MEK1 (10 mg/L), among other factors. The handling of two human signaling enzymes in the context of insect cell intracellular environment remains a key factor for consideration. Different compartmentalization or association with inappropriate insect proteins could certainly hinder efficient phosphorylation. Despite the addition of okadaic acid in the expression media and during lysis, the inhibition of phosphatases in the cell might not have been complete, resulting in partial dephosphorylation. The *in vitro* phosphorylation method using purified GST-cRAF1(Y340D + Y341D) offered more flexibility in optimizing the enzyme substrate ratio, concentrations of Mg^{2+} and ATP, and time and temperature of incubation, allowing the reaction to proceed toward completion in a phosphatase-free environment.

The *in vitro* GST-cRAF1(Y340D + Y341D)-mediated MEK1 activation strategy also provided a robust method for generation of large amounts of activated MEK1 (dubbed as pMEK$^{in\ vitro}$). Given the different extents of phosphorylation levels between the MEK1 preparations, we investigated the binding of allosteric (U0126 and PD0325901) and ATP-competitive inhibitors (K252a and staurosporine) to pMEK1$^{in\ situ}$ and pMEK1$^{in\ vitro}$ proteins for comparison with npMEK1 protein. In thermal shift assay, the pMEK1$^{in\ situ}$ and pMEK1$^{in\ vitro}$ proteins behaved very differently, while the data for pMEK1$^{in\ situ}$ and npMEK1 were largely consistent. The two ATP competitive inhibitors, K252a and staurosporine, bound with higher affinity to pMEK1$^{in\ vitro}$ than its unphosphorylated form (ca. 10- and 4-fold, respectively). In contrast, U0126 and PD0325901 bound pMEK1$^{in\ vitro}$ with a 7−10-fold lower affinity than its unphosphorylated counterpart, npMEK1. The differences in the affinity of the allosteric inhibitors were corroborated across different binding assay formats. In addition to our results, others have reported discrepancies in the

potencies of some of these compounds in various phosphorylation assays involving MEK1. Davies et al. reported decrease in potency of U0126 for MEK-mediated ERK2 phosphorylation (IC50 = 20 μM) compared to RAF1-mediated MEK1 phosphorylation (IC50 = 0.3 μM).[21] Similarly, VanSycoc et al. reported lower potency for U0126 in MEK1-mediated ERK2 catalysis (IC50 = 1.3 μM) compared to RAF1-mediated MEK1 activation (IC50 = 0.17 μM).[20] PD0325901 has only been studied in context of MEK1-ERK2-MBP activation and not RAF1-mediated MEK1 activation.[35] PD098059, another allosteric MEK1 compound, has been shown to preferentially affect RAF1-mediated MEK1 activation rather than MEK1-mediated ERK2 phosphorylation.[22] Taken together, these observations make a compelling case for the preferential binding of allosteric inhibitors to the inactive/unphosphorylated MEK.

The observed TdF K_d for PD0325901 binding to npMEK1, npMEK1·AMP-PnP, pMEK1, and pMEK1·AMP-PnP were 4, 0.009, 27, and 0.2 μM, respectively. Thus, up to 3000-fold difference in PD0325901 affinity could be observed across different MEK1 states. The structural basis of the differences in the binding affinities of apo forms of phosphorylated (TdF K_d = 27 μM) and unphosphorylated MEK1 (TdF K_d = 4 μM) would need high-resolution X-ray structures of npMEK1·PD0325901 and pMEK·PD0325901 complexes for direct comparison. Nonetheless, the structural basis of nucleotide-binding induced increase in affinity for PD0325901 has already been described based on the crystal structure of MEK1·AMP-PnP·PD318088 (an analog of PD0325901). The compound is observed to make a network of stabilizing interactions between nucleotide triphosphate and the protein, which could account for synergistic increase in affinity of the compound in the presence of nucleotide.[17] Although U0126 binds in the same pocket as PD0325901, the binding mode of U0126 is distinct enough not to render any interactions between the inhibitor and nucleotide. This explains the lack of nucleotide effect in the binding of the inhibitor to the nucleotide-bound versus free forms of MEK1 (npMEK1 TdF K_d = 0.7 μM, npMEK1·AMP-PnP TdF K_d = 0.7 μM, pMEK1 TdF K_d = 7 μM, pMEK1·AMP-PnP TdF K_d = 9 μM). Notably though, the phosphorylated MEK1 (TdF K_d = 7 μM) had lower affinity for U0126 compared to its unphosphorylated counterpart (TdF K_d = 0.7 μM). The structural basis of the differences in the affinity of U0126 between the two phosphorylated MEK1 states remains to be elucidated experimentally. Nevertheless, it is important to note that we confirmed the differential binding affinities of the inhibitors to the two forms of the enzyme not by one binding technique but three: thermal denaturation analyses, isothermal calorimetry, and AS-MS. The resulting data converge to the same conclusion and indicate that stoichiometric T-loop phosphorylation and catalytic activation favor the binding of ATP competitive inhibitors represented by K252a and staurosporine, while destabilizing the binding of allosteric inhibitors PD0325901 and U0126.

The intracellular level of activated MEK depends very much on the intensity of receptor stimulation at the cell surface and down the RAS-RAF-MEK-ERK pathway. The effective design of inhibitors that shut down signaling at the MEK level depends in turn on a sound understanding of the mechanism of inhibition of these compounds. As previously discussed, the allosteric type inhibitors developed to date inhibit MEK1 phosphorylation by RAF1 more potently by preferentially binding to the inactive state. In contrast, the ATP-site inhibitors target the phosphorylation of ERK by MEK1 by preferentially binding to activated MEK1. These are the two clear alternatives at hand for medicinal chemists to consider, and we have yet to see a third binding mode where inhibitors could bind with equally high affinity to either states, unphosphorylated or phosphorylated at T-loop. Our current understanding of the exact ratio of active versus inactive MEK at various levels of extracellular receptor stimulation does not allow for a definite prediction of choice between these alternatives. The approach remains empirical and demands exacting tools. The availability of a stoichiometrically activated and highly purified MEK1 preparation is one such tool. It allows for precise *in vitro* characterization of inhibitors by enzymatic assays and direct binding assays using biophysical methods as described herein. It should also be noted that to date all public domain structures of MEK1 reported in the PDB are of the inactive form. This is a clear impediment to iterative structure-based design of inhibitors that preferentially bind the activated form and especially those that do not target the highly conserved ATP site in order to achieve a higher level of selectivity against other kinases. The homogeneously activated MEK1 (pMEK1$^{in\ vitro}$) is certainly a candidate for crystallization experiments and X-ray structure determinations, either in the apo form or in complex with ATP analogs and inhibitors. It is undoubtedly superior to pMEK$^{in\ situ}$ in that respect. Finally, the availability of highly potent MEK1 inhibitors with clearly defined molecular mechanism will facilitate further evaluation of their potency, selectivity, and target engagement at the cellular or higher level.

AUTHOR INFORMATION

Corresponding Author

*Tel: +1 (908) 740-3425. Fax: +1 (908) 740-4844. E-mail: payal.sheth@merck.com.

ABBREVIATIONS

MAP, mitogen activated protein; MKK1 or MEK1, mitogen activated protein kinase kinase 1; ERK1 and ERK2, extracellular signal-regulated kinase 1 and 2; MOI, multiplicity of infection; HRP, horseradish peroxidase; TdF, temperature-dependent fluorescence; AS-MS, affinity-selection mass spectrometry; ITC, isothermal titration calorimetry; pMEK1$^{in\ vitro}$, phosphorylated MEK1 produced by *in vitro* activation by RAF1; pMEK1$^{in\ situ}$, phosphorylated MEK1 produced by coexpression of RAF1 and MEK1 in insect cells; npMEK1, non (T-loop) phosphorylated MEK1; AS-MS, affinity-selection mass spectrometry.

REFERENCES

(1) Corson, L. B., Yamanaka, Y., Lai, K.-M. V., and Rossant, J. (2003) Spatial and temporal patterns of ERK signaling during mouse embryogenesis. *Development 130*, 4527−4537.

(2) Kolch, W. (2005) Coordinating ERK/MAPK signalling through scaffolds and inhibitors. *Nat. Rev. Mol. Cell. Biol. 6*, 827−837.

(3) Wellbrock, C., Karasarides, M., and Marais, R. (2004) The RAF proteins take central stage. *Nat. Rev. Mol. Cell. Biol. 5*, 875−885.

(4) Greenman, C., Stephens, P., Smith, R., Dalgliesh, G. L., Hunter, C., Bignell, G., Davies, H., Teague, J., Butler, A., Stevens, C., Edkins, S., O'Meara, S., Vastrik, I., Schmidt, E. E., Avis, T., Barthorpe, S., Bhamra, G., Buck, G., Chaudhury, B., Clements, J., Cole, J., Dicks, E., Forbes, S., Gray, K., Halliday, K., Harrison, R., Hills, K., Hinton, J., Jenkinson, A., Jones, D., Menzies, A., Mironenko, T., Perry, J., Raine, K., Richardson, D., Shepherd, R., Small, A., Tofts, C., Varian, J., Webb, T., West, S., Widaa, S., Yates, A., Cahill, D. P., Louis, D. N., Goldstraw, P., Nicholson, A. G., Brasseur, F., Looijenga, L., Weber, B. L., Chiew, Y.-

E., deFazio, A., Greaves, M. F., Green, A. R., Campbell, P., Birney, E., Easton, D. F., Chenevix-Trench, G., Tan, M.-H., Khoo, S. K., Teh, B. T., Yuen, S. T., Leung, S. Y., Wooster, R., Futreal, P. A., and Stratton, M. R. (2007) Patterns of somatic mutation in human cancer genomes. *Nature 446*, 153−158.

(5) Roberts, P. J., and Der, C. J. (2007) Targeting the Raf-MEK-ERK mitogen-activated protein kinase cascade for the treatment of cancer. *Oncogene 26*, 3291−3310.

(6) Thiel, M. J., Schaefer, C. J., Lesch, M. E., Mobley, J. L., Dudley, D. T., Tecle, H., Barrett, S. D., Schrier, D. J., and Flory, C. M. (2007) Central role of the MEK/ERK MAP kinase pathway in a mouse model of rheumatoid arthritis: Potential proinflammatory mechanisms. *Arthritis Rheum. 56*, 3347−3357.

(7) Bollag, G., Hirth, P., Tsai, J., Zhang, J., Ibrahim, P. N., Cho, H., Spevak, W., Zhang, C., Zhang, Y., Habets, G., Burton, E. A., Wong, B., Tsang, G., West, B. L., Powell, B., Shellooe, R., Marimuthu, A., Nguyen, H., Zhang, K. Y. J., Artis, D. R., Schlessinger, J., Su, F., Higgins, B., Iyer, R., D'Andrea, K., Koehler, A., Stumm, M., Lin, P. S., Lee, R. J., Grippo, J., Puzanov, I., Kim, K. B., Ribas, A., McArthur, G. A., Sosman, J. A., Chapman, P. B., Flaherty, K. T., Xu, X., Nathanson, K. L., and Nolop, K. (2010) Clinical efficacy of a RAF inhibitor needs broad target blockade in BRAF-mutant melanoma. *Nature 467*, 596−599.

(8) AZD6244/ARRY142886 MEK inhibitor. http://clinicaltrials.gov/ct2/results?term=AZD6244.

(9) RDEA119 and Sorafenib Combination Dose Escalation Study. http://clinicaltrials.gov/ct2/show/NCT00785226?term=RDEA119&rank=1.

(10) Chapman, M. S., Iverson, C., Miampamba, M., Yu, C., Adjei, A. A., Girardet, J.-L., Quart, B., and Miner, J. N. (2009) The selective MEK inhibitor RDEA119: Synergy with multiple classes of anti-cancer agents, in *Proceedings of the 100th Annual Meeting of the American Association for Cancer Research*, AACR, Philadelphia, PA, Denver, CO.

(11) Rosen, L. S., Galatin, P., Fehling, J. M., Laux, I., Dinolfo, M., Frye, J., Laird, D., and Sikic, B. I. (2008) A phase 1 dose-escalation study of XL518, a potent MEK inhibitor administered orally daily to subjects with solid tumors. *J. Clin. Oncol. 26*, xxxx.

(12) Thompson, D. S., Flaherty, K. T., Messersmight, W., Harlacker, K., S., N., Vincent, C., DeMarini, D. J., Cox, D. S., O'Neill, V. J., and Burris, H. A. (2009) A three-part, phase I, dose-escalation study of GSK1120212, a potent MEK inhibitor, administered orally to subjects with solid tumors or lymphoma. *J. Clin. Oncol. 27*, xxxx.

(13) Alessi, D. R., Saito, Y., Campbell, D. G., Cohen, P., Sithanandam, G., Rapp, U., Ashworth, A., Marshall, C. J., and Cowley, S. (1994) Identification of the sites in MAP kinase kinase-1 phosphorylated by p74raf-1. *EMBO J. 13*, 1610−1619.

(14) Zheng, C.-F., and Kun-Liang, G. (1994) Activation of MEK family kinase requires phosphorylation of two conserved Ser/Thr residues. *EMBO J. 13*, 1123−1131.

(15) Chen, Z., Gibson, T. B., Robinson, F., Silvestro, L., Pearson, G., Xu, B.-e., Wright, A., Vanderbilt, C., and Cobb, M. H. (2001) MAP kinases. *Chem. Rev. 101*, 2449−2476.

(16) Friday, B.B., and Adjei, A. A. (2008) Advances in targeting the Ras/Raf/MEK/Erk mitogen-activated protein kinase cascade with MEK inhibitors for cancer therapy. *Clin. Cancer Res. 14*, 342−346.

(17) Fischmann, T. O., Smith, C. K., Mayhood, T. W., Myers, J. E., Reichert, P., Mannarino, A. F., Carr, D., Zhu, H., Wong, J., Yang, R.-S., Le, H. V., and Madison, V. S. (2009) Crystal structures of MEK1 binary and ternary complexes with nucleotides and inhibitors. *Biochemistry 48*, 2661−2674.

(18) Ohren, J. F., Chen, H., Pavlovsky, A., Whitehead, C., Zhang, E., Kuffa, P., Yan, C., McConnell, P., Spessard, C., Banotai, C., Mueller, W. T., Delaney, A., Omer, C., Sebolt-Leopold, J., Dudley, D. T., Leung, I. K., Flamme, C., Warmus, J., Kaufman, M., Barrett, S. D., Tecle, H., and Hasemann, C. A. (2004) Structures of human MAP kinase kinase 1 (MEK1) and MEK2 describe novel noncompetitive kinase inhibition. *Nat. Struct. Mol. Biol. 11*, 1192−1197.

(19) Smith, C. K., and Windsor, W. T. (2006) Thermodynamics of nucleotide and non-ATP-competitive inhibitor binding to MEK1 by circular dichroism and isothermal titration calorimetry. *Biochemistry 46*, 1358−1367.

(20) VanScyoc, W. S., Holdgate, G. A., Sullivan, J. E., and Ward, W. H. J. (2008) Enzyme kinetics and binding studies on inhibitors of MEK protein kinase. *Biochemistry 47*, 5017−5027.

(21) Davies, S. P., Reddy, H., Caivano, M., and Cohen, P. (2000) Specificity and mechanism of action of some commonly used protein kinase inhibitors. *Biochem. J. 351*, 95−105.

(22) Alessi, D. R., Cuenda, A., Cohen, P., Dudley, D. T., and Saltiel, A. R. (1997) PD 098059 is a specific inhibitor of the activation of mitogen-activated protein kinase kinase in vitro and in vivo. *J. Biol. Chem. 270*, 27489−27494.

(23) Favata, M.F., Horiuchi, K. Y., Manos, E. J., Daulerio, A. J., Stradley, D. A., Feeser, W. S., Van Dyk, D. E., Pitts, W. J., Earl, R. A., Hobbs, F., Copeland, R. A., Magolda, R. L., Scherle, P. A., and Trzaskos, J. M. (1998) Identification of a novel inhibitor of mitogen-activated protein kinase kinase. *J. Biol. Chem. 273*, 18623−18632.

(24) Smith, C. K., Carr, D., Mayhood, T. W., Jin, W., Gray, K., and Windsor, W. T. (2007) Expression and purification of phosphorylated and non-phosphorylated human MEK1. *Protein Expression Purif. 52*, 446−456.

(25) Matulis, D., Kranz, J. K., Salemme, F. R., and Todd, M. J. (2005) Thermodynamic stability of carbonic anhydrase: measurements of binding affinity and stoichiometry using ThermoFluor. *Biochemistry 44*, 5258−5266.

(26) Pantoliano, M. L., Petrella, E. C., Kwasnoski, J. D., Lobanov, V. S., Myslik, J., Graf, E., Carver, T., Asel, E., Springer, B. A., Lane, P., and Salemme, F. R. (2001) High-density miniaturized thermal shift assays as a general strategy for drug discovery. *J. Biomol. Screen. 6*, 429−440.

(27) Sheth, P. R., Ramanathan, L., Ranchod, A., Basso, A. D., Barrett, D., Zhao, J., Gray, K., Liu, Y.-H., Zhang, R., and Le, H. V. (2010) Expression, purification, stability optimization and characterization of human Aurora B kinase domain from E. coli. *Arch. Biochem. Biophys. 503*, 191−201.

(28) Zhang, R., and Monsma, F. (2010) Fluorescence-based thermal shift assays. *Curr. Opin. Drug Discovery Dev. 13*, xxxx.

(29) Annis, D. A., Athanasopoulos, J., Curran, P. J., Felsch, J. S., Kalghatgi, K., Lee, W. H., Nash, H. M., Orminati, J.-P. A., Rosner, K. E., Shipps, G. W. Jr., Thaddupathy, G. R. A., Tyler, A. N., Vilenchik, L., Wagner, C. R., and Wintner, E. A. (2004) An affinity selection-mass spectrometry method for the identification of small molecule ligands for self-encoded combinatorial libraries: Discovery of a novel antagonist of E. coli dihydrofolate reductase. *Int. J. Mass Spectrom. 238*, 77−83.

(30) Annis, D. A., Shipps, G. W. Jr., Deng, Y., Popovici-Muller, J., Siddiqui, M. A., Curran, P. J., Gowen, M., and Windsor, W. T. (2007) Method for quantitative protein-ligand affinity measurements in compound mixtures. *Anal. Chem. 79*, 4538−4542.

(31) Sheth, P. R., Shipps, G. W. Jr., Seghezzi, W., Smith, C. K., Chuang, C.-C., Sanden, D., Basso, A. D., Vilenchik, L., Gray, K., Annis, D. A., Nickbarg, E., Ma, Y., Lahue, B., Herbst, R., and Le, H. V. (2010) Novel benzimidazole inhibitors bind to a unique site in the kinesin spindle protein motor domain. *Biochemistry 49*, 8350−8358.

(32) Frost, J. A., Steen, H., Shapiro, P., Lewis, T., Ahn, N., Shaw, P. E., and Cobb, M. H. (1997) Cross-cascade activation of ERKs and ternary complex factors by Rho family proteins. *EMBO J. 16*, 6426−6438.

(33) Eblen, S. T., Slack-Davis, J. K., Tarcsafalvi, A., Parsons, J. T., Weber, M. J., and Catling, A. D. (2004) Mitogen-activated protein kinase feedback phosphorylation regulates MEK1 complex formation and activation during cellular adhesion. *Mol. Cell. Biol. 24*, 2308−2317.

(34) Eblen, S. T., Slack, J. K., Weber, M. J., and Catling, A. D. (2002) Rac-PAK signaling stimulates extracellular signal-regulated kinase (ERK) activation by regulating formation of MEK1-ERK complexes. *Mol. Cell. Biol. 22*, 6023−6033.

(35) Barrett, S. D., Bridges, A. J., Dudley, D. T., Saltiel, A. R., Fergus, J. H., Flamme, C. M., Delaney, A. M., Kaufman, M., LePage, S., Leopold, W. R., Przybranowski, S. A., Sebolt-Leopold, J., Becelaere, K. V., Doherty, A. M., Kennedy, R. M., Marston, D., Howard, W. A. J.,

Smith, Y., and Warmus, J. S. (2008) The discovery of the benzhydroxamate MEK inhibitors CI-1040 and PD 0325901. *Bioorg. Med. Chem. Lett. 18*, 6501−6504.